Optical filter assembly for interplanetary optical communications

Yijiang Chen and Hamid Hemmati

Jet Propulsion Laboratory, California Institute of Technology, Pasadena, CA 91109

ABSTRACT

Ground-based, narrow-band, high throughput optical filters are required for optical links from deep space. We report on the development of a tunable filter assembly that operates at telecommunication window of 1550 nm. Low insertion loss of 0.5 dB and bandwidth of 90 pm over a 2000 nm operational range of detectors has been achieved.

Key Words: Optical communications, Optical filters

1. INTRODUCTION

Detection of extremely faint optical signals originated at interplanetary distances requires Earth-based telescopes with an effective diameter on the order of 10m in conjunction with high detection efficiency photon counting detectors [1,2]. Narrow-band low-insertion loss optical filters are required to efficiently separate signal photons from out-of-band background noise photons over a wide spectral response region of the photodetector. Such filters are not available off-the-shelf, prompting a custom development.

Superconducting nanowire detectors are presently the best candidate for photon starved optical communications at near-infrared optical communications wavelengths [3]. Current key nanowire photon-counting candidates are: the niobium nitride (NbN and NbTiN) superconductors [4-6], and the superconducting amorphous tungsten–silicon alloy (a-W_xSi_{1-x}) detectors [7]. The latter has been demonstrated to have a detector system efficiency of 19%–40% over a wavelength range of 1280–1650 nm [7], which is an improvement compared with the conventional fiber-coupled NbN SNSPDs with an efficiency of 10% [8, 9]. By adding an optical cavity to NbN nanowire detectors, the detection efficiencies of the integrated nano-electro-photonic devices were improved significantly [10]. With implementation of such an integration scheme for superconducting a-W_xSi_{1-x} nanowire detectors, the detection efficiencies of the a-W_xSi_{1-x} nanowire devices were increased significantly as well (80% ~ 93%) [11]. On the other hand, the a-W_xSi_{1-x} device requires lower operation temperature below 1 K, whereas nitride superconductor single photon detectors operate at 3 K. Despite their distinctive features, both NbN and a-W_xSi_{1-x} devices have wide spectral response from visible to infrared. Figure 1 shows the calculated spectral characteristic of tungsten–silicon alloy nanowire.

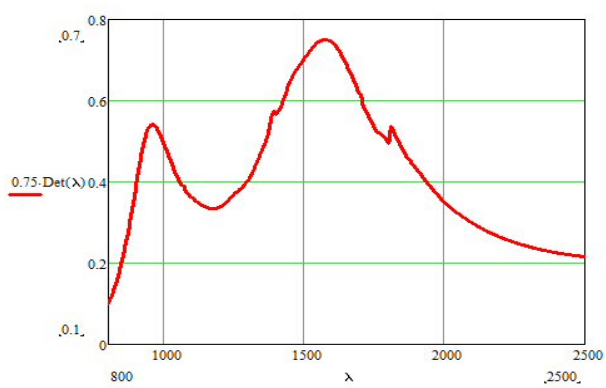

Figure 1. Calculated spectral response of tungsten–silicon alloy nanowire

Here, we report on the development of a low-loss narrow-band filter for deep space optical links. A survey of existing filter technologies indicated that there are no existing single filter technologies or off-the-shelf parts that are capable of meeting the pre-set requirements. Options of combining different filter technologies to meet the requirements were explored. Four options were constructed to meet the requirements and an option was down-selected for laboratory implementation.

2. REQUIREMENTS

Based on the flight terminal transmitter and orbital operation requirements, ground receiver design and Earth atmospheric effect, the ground receiver filter requirements are derived and shown in Table 1.

Table 1. Ground optical receiver filter requirements

Parameters	Requirement	Justification
Center wavelength (nm)	~1550	DOT requirement
Tunability (pm)	±150	• ±80 pm, from expected post-launch shift (10% ITU grid of 100GHz) • ±40 pm, from max Doppler shift • ±10 pm (=0.1*dλ/dT), from laser chamber temperature drift of 0.1° C • ±20 pm, assumed margin
Bandwidth (noise equivalent - nm)	0.17±0.03	DOT requirement
Transmission efficiency (%)	>80	DOT requirement
Minimum clear aperture (mm)	>23	To cover 2 to 12m telescope apertures; and FOV=50 μrad of atmospheric seeing for daytime operation (DOT require. L3-GLR3.8)
Acceptance angle (FOV - degree)	≥1.5	Same as above
dλ/dT (pm/° C)	>10 <85	Not too small requiring large temperature variation for tuning, but not too large causing big change with small temperature variation (instability)
Out-of-band rejection range (nm)	1,000 to 3,000	Nanowire detector has response over all the wavelengths with peak around 1550nm. BK7 or silica will be placed in front of the detector to remove noise/unwanted signals below 0.3μm and above 3μm
Ratio of integrated power within the signal band to that outside the signal band	>3 or 10	Contributions (radiance, stray light, noise) outside the band can be comparable to those within the band, because photon counting detectors follow Poisson statistics
Operating temperature (° C)	5 to 80	Temperature likely experienced by filter
Surface quality (scratch & dig)	40-10	Negligible scattering
Surface flatness (at 633nm)	<λ/4	Negligible scattering
Polarization	Meet spec for any polarization	Depolarization/polarization must be less than 1%

The rationale for key requirements is described below.

a. **Center wavelength:** The center wavelength of the filter system is specified at 1550.12 nm. This wavelength lies within terrestrial optical fiber communication window; system components such as lasers and amplifiers at this wavelength are well developed and widely available from numerous commercial vendors. Therefore, less effort will be needed to adapt the commercialized components for deep space applications, mainly on environmental adaptability.

b. **Bandwidth:** Noise equivalent bandwidth of the filter is specified for 0.17 nm [1,2]. The downlink signal bandwidth is actually 2 pm or less, much narrower than this requirement. Theoretically, the filter system bandwidth requirement can be reduced to 17 pm or less, i.e., at least by an order of magnitude; still the downlink signal will get through the filter system while unwanted noise is rejected, provided the filter center wavelength is aligned with the signal center wavelength. However, a filter spectral bandwidth narrower than the current requirement may impose practical limitation for fabrication and wavelength tuning requirements to precisely match the filter center wavelength with the signal center wavelength.

c. **Transmission efficiency:** Minimum insertion loss from the filter system is desired, so that the signal experiences negligible loss while passing through the filter system. Based on down link budget [1], 75% of the input signal must be recovered at the output of the filter system. Allowing adequate margin for the downlink budget, the transmission efficiency is specified as 80%. Further increase in the transmission efficiency for the requirement may impose great difficulty for fabrication of the very narrow band filters.

d. **Ratio of integrated power within the signal band to that outside the signal band:** The response of the detector is the accumulation or integral of all the signals within its spectral sensitive region. Figure 1 is the nanowire detector response spectrum and Figure 2 is sky radiance used for the ratio estimation. Although out of band noise (e.g., radiance and stray light) is attenuated by 30 dB to 40 dB upon transmission through the filter, the large spectral bandwidth of the detector can still make significant contribution to the overall number of detected noise relative to

detected in-band signal. To avoid the interference of the out-of-band unwanted background noise to the in-band transmitted signal, total outside band contributions must be at least less than one third of the signal within the transmission band, as photon counting detectors follow Poisson statistics with PPM channel capacity proportional to signal photon square divided by noise photons. The ratio of integrated power within the signal band to that outside the signal band is preferred to be greater than 10. However, high suppression ratio requirement results in more challenging filter fabrication. .

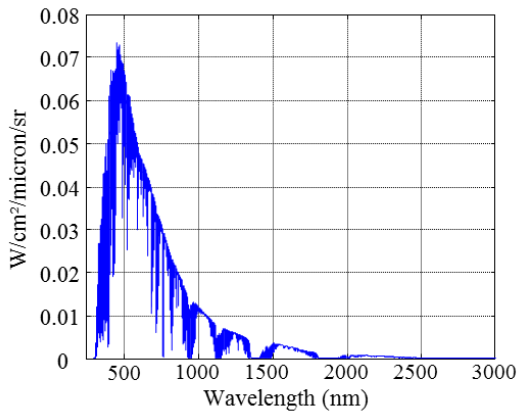

Figure 2. Sky radiance used for suppression ratio estimation

3. RELEVANT FILTER TECHNOLOGIES

Suitable ingredients for filter assembly include: dielectric interference filters, Fabry-Perot Etalon (FPE) filters, and Volume Bragg Grating (VBG) filters. The dielectric interference filter can be designed for high quality filtering over approximately a 200nm range (Fig.3a), but it is difficult to fabricate for uniformity along with high transmission efficiency, especially when deposition of many thin film layers is required. Fabry-Perot Etalon filters, on the other hand, are simpler to fabricate, but their free spectral range is typically a limitation (Fig.3b). Volume Bragg Grating provides high quality filtering within the transmission band, but its side lobes outside the transmission band (Fig.3c) influence suppression of unwanted out-band noise.

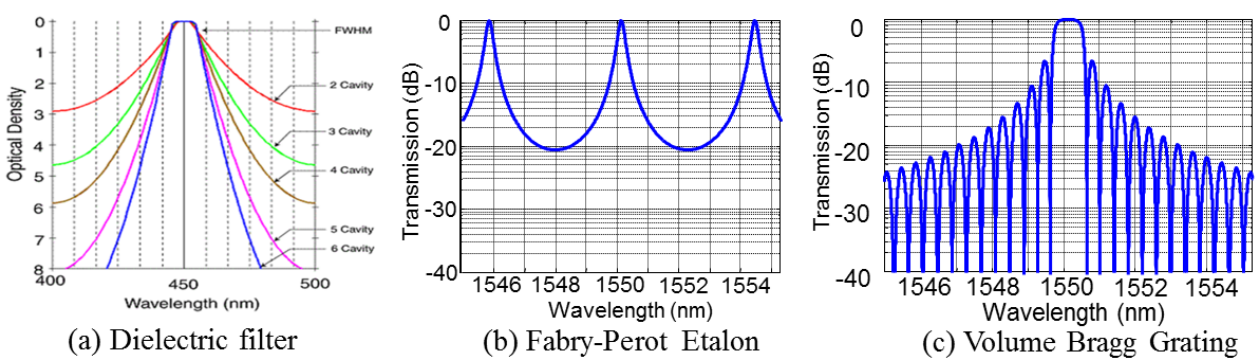

Figure 3. Spectral responses of three filters

Any single filter listed in Figure 3 clearly cannot meet the requirements of Table 1 for our ground receiver terminal. The current solution is to develop a new filter assembly with single filter configuration that can meet the requirements or to devise combinations of existing filter technologies to meet the requirements. We resorted to the latter approach.

4. OPTIONS FOR COMBIED FILTER TECHNOLOGIES

Table 2 lists four options for various combinations of the existing filter technologies to meet the requirements of Table 1.

Table 2. Options & cost with available technology to meet the requirements

Parameters	Requir.	A) #1 (VBG)	B) #2 (VBG)	C) #1 (FEP)	D) #2 (FEP)	E) (Interference)	F) (Wide band)	G) (Long wave blocking)	Option 1 A+C+G	Option 2 A+E+G	Option 3 E+F+G	Option 4 C+F+G
Center wavelength (nm)	1550	1550	1550	1550	1550	1550	1550	1550	1550	1550	1550	1550
Tunability (pm)	±150	±150	±150	±150	±150	±150	N/A	N/A	±150	±150	±150	±150
Bandwidth (nm)	0.17	0.2	0.15	0.17	0.17	0.17	3	>50	0.17	0.17	0.17	0.17
Transmission efficiency (%)	>80	96	93	95	97	>80 (85)	95	95	87 (-0.6dB)	78 (-1.08dB)	77 (-1.14dB)	86 (-0.66dB)
Minimum clear aperture (mm)	>23	23	23	23	23	23	23	23	23	23	23	23
Acceptance angle (FOV - mrad)	>26	24	24	24	24	24	24	24	24	24	24	24
dλ/dT (at 0.1°C tem. variation)	>9pm/°C <85 pm/°C	15	15	9	9	13	N/A	N/A	15/9	15/13	13	9
Out of band rejection range (nm)	850-3000	800-2800	800-2800	4	4	1380-1770	850-1780	1750-3000	850-3000	850-3000	850-3000	850-3000
Out of band rejection ratio	>10	<1	<1	<1	<1	<1	<1	<1	7	12	3.7	1
Price ($K)		30.9	36.4	14.3	14	66.4	0.622	3.5	48.7	100.8	70.522	18.122
Lead time (Weeks)	16	8-12	8-12	10-12	5	16	1	8	10-12	16	16	10-12
Required ovens	1	1	1	1	1	1	0	0	2	2	1	1

Option 1 is a combination of VBG, FP and Long wave blocking filter. The use of FP is to suppress the side-lobe effect of VBG and Long wave blocking filter (Fig. 4c) complements ineffectiveness of VBG beyond 2800 nm (Fig. 4a). Figure 5 is the filter response of Option 1 with combination of VBG, FP and Long wave blocking filter. The spectral characteristic from 1000 nm to 3000 nm is shown in Figure 5a and an expanded version of the spectral characteristic from 1549.4 nm to 1551 nm is given in Figure 5b.

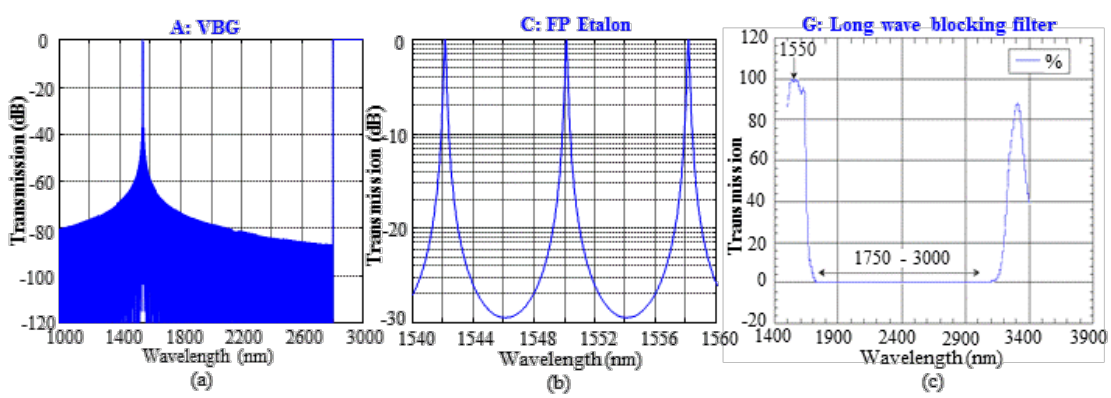

Figure 4. Spectral responses of each individual filter for Option 1

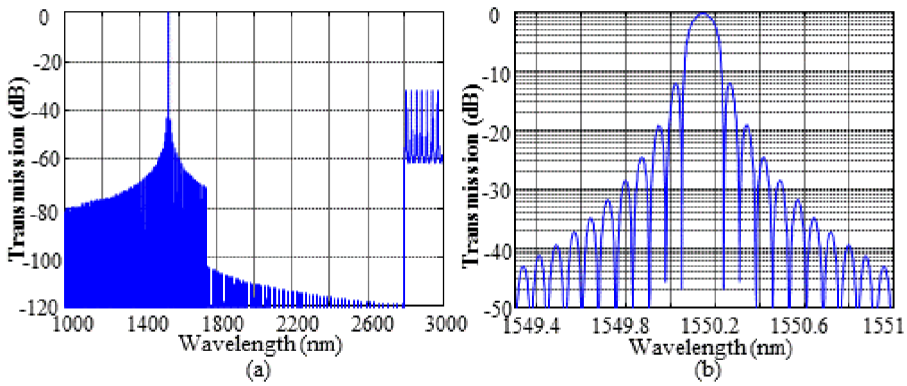

Figure 5. Spectral response of Option 1

Option 2 is similar to Option 1, but with FP replaced by the dielectric filter. The dielectric filter (Fig. 6a) removes the side-lobe effect of VBG. The spectral response of Option 2 is shown in Figure 6b (from 1000 nm to 3000 nm) and Figure 6c (from 1549.4 nm to 1551 nm). The principal differences between Option 1 and Option 2 are out-band rejection ratio, transmission efficiency and cost. Option 2 gives out-of-band rejection ratio of 12 versus 7 for Option 1, but the transmission efficiency for Option 2 is reduced to 78% compared to 87% for Option 1. Cost, which may not be a main concern, for Option 2 is also higher than that for Option 1. These features and differences are listed in Table 2.

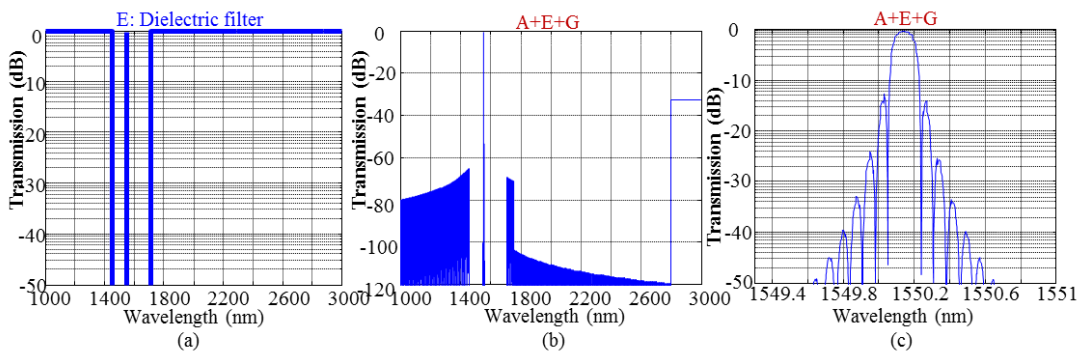

Figure 6. (a) Individual dielectric filter response; (b) and (c) Spectral response of Option 2

Option 3 is a combination of dielectric filter, 3 nm wide band filter and Long wave blocking filter. The wide band filter helps to overcome the limitation of operation of dielectric filter within 200 nm range and Long wave blocking filter complements ineffectiveness of 3 nm wide band filter beyond 1800 nm as shown in Figure 7a. Figures 7b and 7c are the spectral response of Option 3 from 1000 nm to 3000 nm and 1549.4 nm to 1551 nm respectively. This option gives lower out-of-band rejection ratio of 3.7 and transmission efficiency of 77% than those of Options 1 and 2.

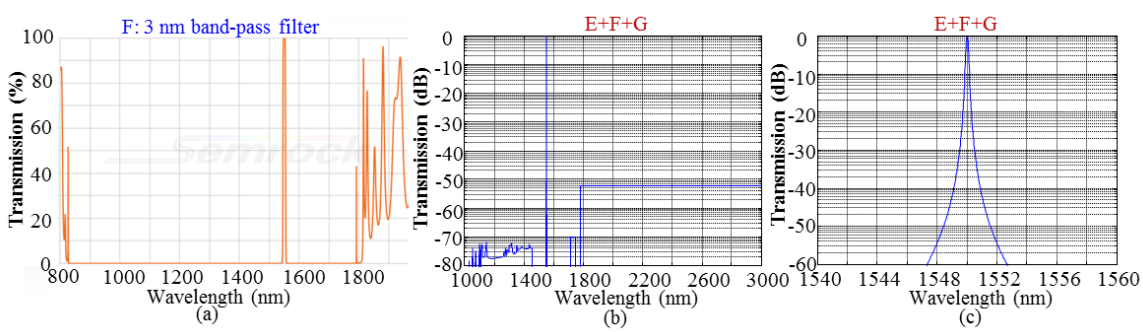

Figure 7. (a) 3 nm wide band filter spectral response; (b) and (c) Spectral response of Option 3

The last option is a combination of FPE, 3 nm wide band filter, and Long wave blocking filter. The spectral response is shown in Fig. 8. This option is a lower cost version, and out-band suppression ratio may be too low to meet the requirement.

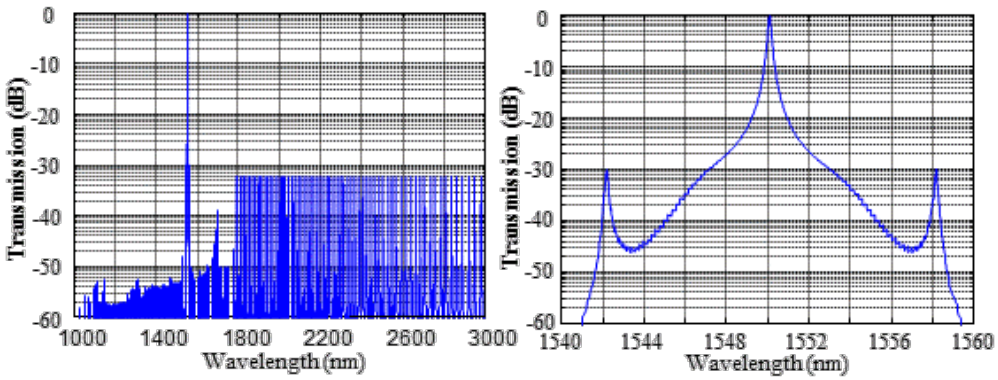

Figure 8. Spectral response of Option 4

5. LABORATORY IMPLEMENTION

We chose to implement Option 1 since it closely met most requirements. Figure 9a is the block diagram of the filter assembly as implemented for characterization. The 1550 nm signal goes through a polarization controller (PC), which compensates polarization distortion of the signal beam while transmitting through the Earth atmosphere for a linearly polarized beam. PC is controlled and adjusted by the feedback signal from leakage of a polarizing-beam-splitter (PBS) in the beam path. The signal then passes through a quarter-wave-plate (QWP) before being reflected from VBG. The signal beam is then routed to FP from VBG through QWP and PBS. Both VBG and FP are placed in temperature chambers for the filter center wavelength tunings to track the down link signal center wavelength change due to, e.g., the Doppler effect. In our proof-of-concept demonstration, PC's polarization control and oven temperature adjustments are achieved manually.

The configuration of Figure 9a was built up in our laboratory. Figure 9b is the setup photo of the experiment. Before integration of the parts, FP and VPG were characterized. The measured results for FP are shown in Figure 10. The bandwidth of the FP is 150 pm (Fig. 10b) with free spectral range of 4 nm (Fig. 10a). Transmission efficiency is 94% and temperature coefficient for wavelength tuning is $|d\lambda/dT|=3.4$ pm/^{o}C (Fig. 10c). This temperature tuning coefficient is lower than the requirement >9 pm/^{o}C. The reason is that the FP is made of ULE. By replacing ULE with other materials of high thermal expansion coefficient such as silica, the temperature-tuning coefficient of FP will fall within the requirement range.

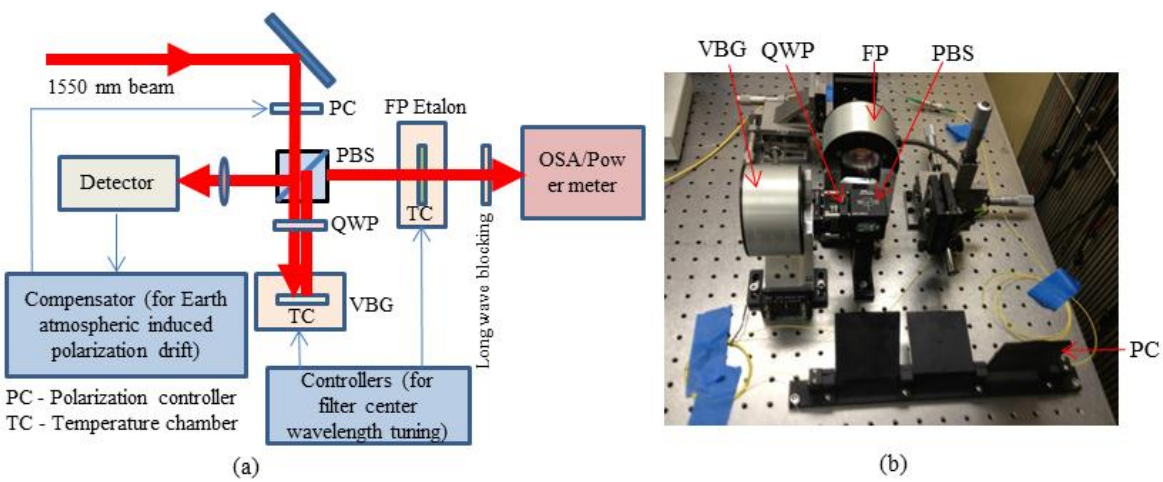

Figure 9. (a) Block diagram of experimental implementation of Option 1; (b) Experimental setup photo

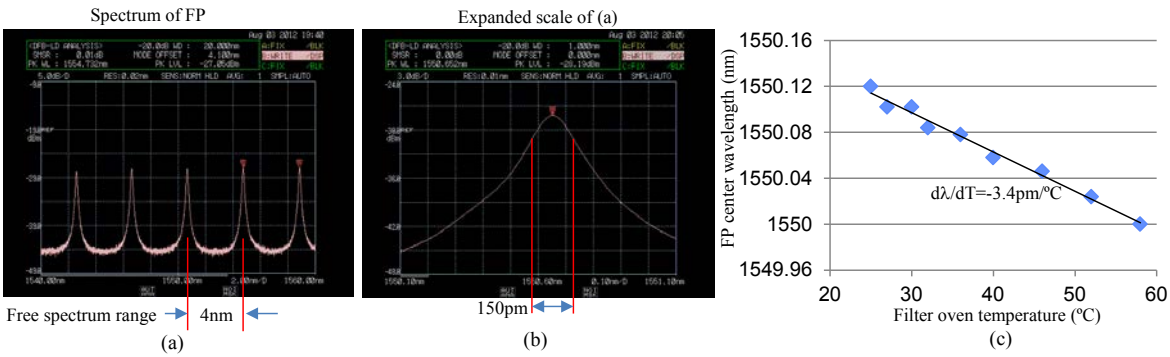

Figure 10. (a) Measured spectrum of FP; (b) Expanded scale of (a); (c) Measured wavelength vs temperature variation coefficient

Figure 11 summarizes the results of VBG's characterization. The measured bandwidth is 140 pm (Fig. 11a) and transmission efficiency is 94%. The temperature variation coefficient is $|d\lambda/dT|$=13 pm/^{o}C (Fig. 11b), meeting the requirement. At the desired center wavelength 1550.12 nm, the chamber temperature is 58°C. The preferred oven temperature at 1550.12 nm is around 45°C, so that the chamber temperature does not have to rise above 70°C for 150 pm tuning range.

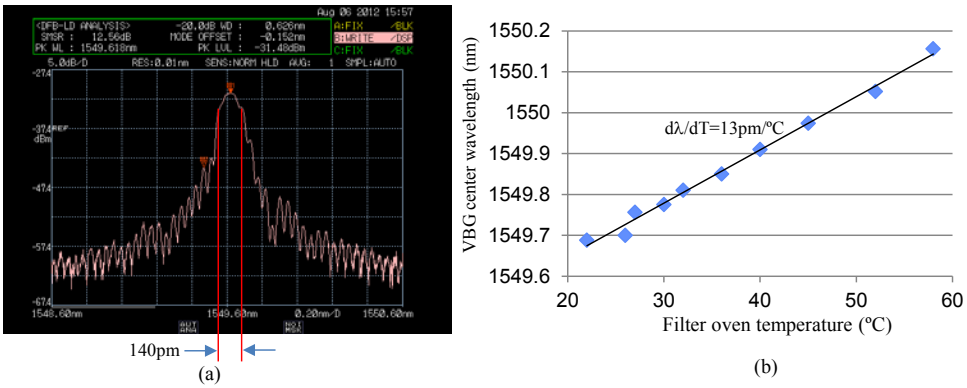

Figure 11. (a) Spectrum of VBG; (b) Measured wavelength vs temperature variation coefficient

The experimental results of the combined operation of VBG and FP are shown in Figure 12. The measured bandwidth is 90 pm and the transmission efficiency is 88.4% or the insertion loss is 0.5 dB. Figure 12a is a scope trace of the spectrum and Figure 12b is the spectrum of the combination of VBG and FP along with individual FP and VBG.

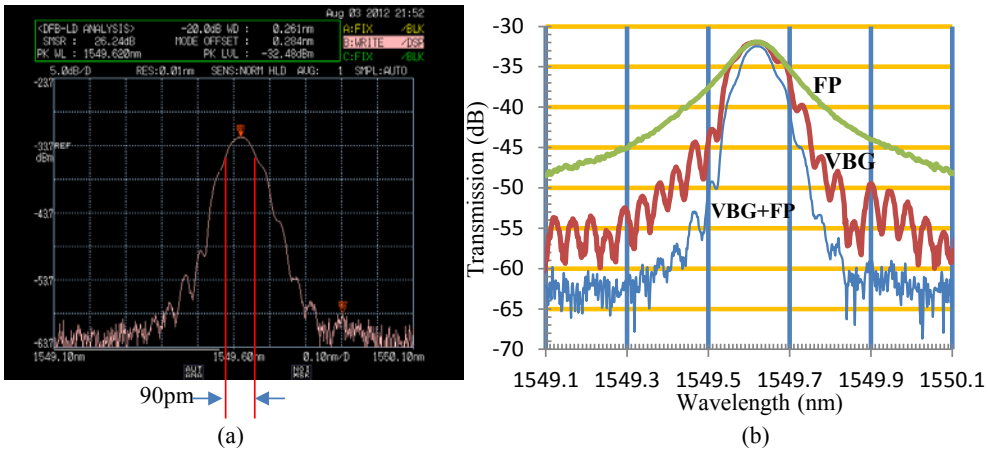

Figure 12. Spectrum of combination of VBG with FP.

6. CONCLUSION

An optical filter assembly suitable for interplanetary optical communications is described. This filter has a band-pass of 90 pm over a large 2000 nm operational range at telecommunication window of 1550 nm. Future work includes: design and fabrication of FP with material having large thermal coefficient; design and fabrication of VBG with center wavelength of 1550.12 nm at temperature around 45°C; automatic temperature tunings of FP and VBG filter center wavelengths for tracking the downlink signal wavelength; automation of PC for polarization compensation; custom filter ovens for automation of wavelength tuning and lifting temperature tunable range from current 60°C to 80°C; and exploration of Option 2 for implementation with better out-band rejection ratio and transmission efficiency.

Acknowledgements: We are grateful to Jeffry Stern and William Farr of JPL for very helpful suggestions. The work described here was performed at the Jet Propulsion Laboratory (JPL), California Institute of Technology under contract with the National Aeronautics and Space administration (NASA).

REFERENCES

[1] Biswas, A., Hemmati, H., Piazzolla, S., Moision, B., Birnbaum, K. and Quirk, K., "Deep-space Optical Terminals (DOT) Systems Engineering", IPN Progress Report 42-183, November 15, 2010.

[2] Farr, W., Regehr, M., Wright, M., Sheldon, D., Sahasrabudhe, A., Gin J., and Nguyen, D., "Overview and Design of the DOT Flight Laser Transceiver", IPN Progress Report 42-185, May 15, 2011.

[3] Farr, W., Stern, J., Shaw, M. D. "Superconducting nanowire arrays for multi-meter free space optical communications receivers", Proc. of SPIE Vol. 8246, 82460R , 2012.

[4] Gol'tsman, G. N., Okunev, O., Chulkova, G., Lipatov, A., Semenov, A. Smirnov, K., Voronov, B. and Dzardanov, A., "Picosecond superconducting single-photon optical detector", Appl. Phys. Lett. **79**, 705, 2001.

[5] Hadfield, R. H., "Single-photon detectors for optical quantum information applications", Nat. Photonics. **3**, 696, 2009.

[6] Verevkin, A., Zhang, J., Sobolewski, R., Lipatov, A., Okunev, O., Chulkova, G., Korneev, A., Smirnov, K., Gol'tsman G. N., "Detection efficiency of large-active-area NbN single-photon superconducting detectors in the ultraviolet to near-infrared range", Appl. Phys. Lett. **80**, 4687, 2002.

[7] Baek, B., Adriana, E. L., Verma, V., Nam, S. W., "Superconducting a-WxSi1−x nanowire single-photon detector with saturated internal quantum efficiency from visible to 1850nm", Appl. Phys. Lett. **98**, 251105, 2011.

[8] Hadfield, R. H., Stevens, M. J., V., Gruber S. S., Miller, A. J. Schwall, R. E,. Mirin, E. P., Nam, S. W. "Single photon source characterization with a superconducting single photon detector", Opt. Express. **13**, 10846, 2005.

[9] Baek, B., Stern, J. A., V., Nam S. W., "Superconducting nanowire single-photon detector in an optical cavity for front-side illumination", Appl. Phys. Lett. **95**, 191110, 2009.

[10] Rosfjord, K. M., Yang, J. K. W., Dauler, E. A., Kerman, A. J., Anant, V., Voronov, B. M., Gol'tsman, G. N., Berggren, K. K. "Nanowire Single-photon detector with an integrated optical cavity and anti-reflection coating", Opt. Express. **14**, 527, 2006.

[11] Marsili, F., Verma, V. B., Stern, J. A., Harrington, S., Lita, Gerrits, A. E., Vayshenker T., I., Baek, B., Shaw, M. D., Mirin, R. P., and Nam , S. W., "Detecting single Infrared photons with 93% system efficiency", www.arxiv.org, arXiv:1209.5774.

.